Triple inhibition of EGFR, Met, and VEGF suppresses regrowth of HGF-triggered, erlotinib-resistant lung cancer harboring an *EGFR* mutation

Junya Nakade, MS,* Shinji Takeuchi, MD, PhD,* Takayuki Nakagawa, MS,* Daisuke Ishikawa, MD,* Takako Sano, PhD,* Shigeki Nanjo, MD,* Tadaaki Yamada, MD, PhD,* Hiromichi Ebi, MD, PhD,* Lu Zhao, MS,* Kazuo Yasumoto, MD, PhD,* Kunio Matsumoto, PhD,† Kazuhiko Yonekura, PhD,‡ and Seiji Yano, MD, PhD*

*Division of Medical Oncology, Cancer Research Institute, Kanazawa University, 13-1 Takara-machi, Kanazawa, Ishikawa 920-0934, Japan; †Division of Tumor Dynamics and Regulation, Cancer Research Institute, Kanazawa University, Kakuma-machi, Kanazawa, Ishikawa 920-1192, Japan; ‡ Tsukuba Research Center, Taiho Pharmaceutical, Co. Ltd., Tsukuba, Ibaraki 300-2611, Japan

To whom correspondence should be addressed.
Seiji Yano, MD, PhD
Division of Medical Oncology, Cancer Research Institute, Kanazawa University, 13-1 Takara-machi, Kanazawa, Ishikawa 920-0934, Japan.
Phone: +81-76-265-2780
Fax: +81-76-234-4524
E-mail: syano@staff.kanazawa-u.ac.jp

Conflicts of Interest and Source of Funding:
S. Yano received honoraria from Chugai Pharma and AstraZeneca and research funding from Chugai Pharma. T. Nakagawa is an employee of Eisai Co., Ltd. K. Yonekura is an employee of Taiho Pharmaceutical Co., Ltd. The other authors have no potential conflicts of interest to disclose.

Grant support: This study was supported by Grants-in-Aid for Cancer Research (21390256 to S.Y.); Scientific Research on Innovative Areas "Integrative Research on Cancer Microenvironment Network" from the Ministry of Education, Culture, Sports, Science and Technology of Japan (22112010A01 to S.Y.); and Taiho Pharmaceutical, Co. Ltd.

Key words: HGF, VEGF, EGFR-TKI resistance, lung cancer, EGFR mutation

Abstract

Purpose: Met activation by gene amplification and its ligand, hepatocyte growth factor (HGF), imparts resistance to epidermal growth factor receptor (EGFR) tyrosine kinase inhibitors (TKIs) in *EGFR*-mutant lung cancer. We recently reported that Met activation by HGF stimulates vascular endothelial growth factor (VEGF) production and facilitates angiogenesis, which indicates that HGF induces EGFR-TKI resistance and angiogenesis. This study aimed to determine the effect of triple inhibition of EGFR, Met, and angiogenesis on HGF-triggered EGFR-TKI resistance in *EGFR*-mutant lung cancer.

Experimental design: Three clinically approved drugs, erlotinib (an EGFR inhibitor), crizotinib (an inhibitor of anaplastic lymphoma kinase and Met), and bevacizumab (anti-VEGF antibody), and TAS-115, a novel dual TKI for Met and VEGF receptor 2 (VEGFR-2) were used in this study. *EGFR*-mutant lung cancer cell lines, PC-9, HCC827, and *HGF*-gene transfected PC-9 (PC-9/HGF) cells were examined.

Results: Crizotinib and TAS-115 inhibited Met phosphorylation and reversed erlotinib resistance and VEGF production triggered by HGF in PC-9 and HCC827 cells *in vitro*. Bevacizumab and TAS-115 inhibited angiogenesis in PC-9/HGF tumors *in vivo*. Moreover, the triplet erlotinib, crizotinib, and bevacizumab, or the doublet erlotinib and TAS-115 successfully inhibited PC-9/HGF tumor growth and delayed tumor regrowth associated with sustained tumor vasculature inhibition even after cessation of the treatment.

Conclusions: These results suggest that triple inhibition of EGFR, HGF/Met, and VEGF/VEGFR-2, by either a triplet of clinical drugs or TAS-115 combined with erlotinib may be useful for controlling progression of *EGFR*-mutant lung cancer by reversing EGFR-TKI resistance and for inhibiting angiogenesis.

Abbreviations: ALK, Anaplastic lymphoma kinase; EML4, Echinoderm microtubule-associated protein-like 4; EGF, Epidermal growth factor; EGFR, Epidermal growth factor receptor; EGFR-TKI, EGFR tyrosine kinase inhibitor; HGF, hepatocyte growth factor; Met-TKI, Met tyrosine kinase inhibitor; NSCLC, Non-small cell lung cancer; SCLC, Small cell lung cancer; VEGF, vascular endothelial growth factor

Introduction

Lung cancer is the leading cause of cancer-related deaths worldwide. Recent advances in molecular biology have identified driver oncogenes such as epidermal growth factor receptor (EGFR) mutations or the echinoderm microtubule-associated protein-like 4 (EML4)/anaplastic lymphoma kinase (ALK) fusion gene in non-small cell lung cancer (NSCLC). In the treatment of NSCLCs harboring these driver oncogenes, the use of EGFR tyrosine kinase inhibitors (EGFR-TKIs; gefitinib and erlotinib) and an ALK inhibitor (crizotinib) to block driver oncogene survival signals resulted in marked tumor regression (1-4). In spite of these clinical successes, tumors acquire resistance to those agents in almost all cases during the course of therapy (5).

Recently, several mechanisms of EGFR-TKI resistance have been identified and classified as follows: 1) alteration of the target *EGFR* gene (e.g., T790M gatekeeper mutation (6,7)); 2) activation of bypass resistance signals (e.g., *Met* gene amplification (8), HGF overexpression (9), and activation of the NFkB pathway (10) and Gas6-AXL axis (11)); and 3) other mechanisms such as transformation to small cell lung cancer (SCLC) (12-14), epithelial-to-mesenchymal transition (15-17), alteration of microRNA (18), and downregulation of MED12 (19). Previously, we demonstrated that HGF activates, via the Met/PI3K/Akt pathway, bypass signals that trigger resistance; overexpression of HGF was observed more frequently than T790M and *Met* amplification in tumors from NSCLC patients who acquired EGFR-TKI resistance in a Japanese cohort (20). These findings indicate that HGF is a clinically relevant target for overcoming EGFR-TKI resistance in *EGFR*-mutant lung cancer.

Angiogenesis is essential for the progression of various types of solid tumors, including NSCLC. Vascular endothelial growth factor (VEGF) is the most prominent pro-angiogenic molecule and is considered to be a therapeutic target in NSCLC. We previously reported that overexpressed HGF stimulates VEGF production via phosphorylation of Met/Gab1 and promotes tumor growth by stimulating angiogenesis in *EGFR*-mutant lung cancer models (21), which indicates that HGF is a critical inducer of not only EGFR-TKI resistance but also angiogenesis in *EGFR*-mutant lung cancer. Therefore, we hypothesized that triple inhibition of the driver signal (EGFR), bypass

resistance signal (Met), and angiogenesis (VEGF) may be beneficial for controlling the progression of *EGFR*-mutant lung cancer with HGF-triggered EGFR-TKI resistance.

As molecularly targeted drugs, EGFR-TKIs, erlotinib, gefitinib, ALK-TKI, crizotinib, and the anti-VEGF antibody bevacizumab have been clinically approved in many countries. Crizotinib is known to have activity against Met in addition to ALK and ROS1 (22-23). In the present study, we investigated the therapeutic effect of triple inhibition against HGF-triggered, EGFR-TKI–resistant lung cancer harboring an *EGFR* mutation by using clinically available targeted drugs, namely, erlotinib, crizotinib, and bevacizumab. We further assessed the therapeutic potential of erlotinib and TAS-115 (Supplemental Figure 1), a novel VEGFR-2 inhibitor, which can be orally administered and has Met inhibitory activity, and we compared this doublet treatment with the clinically available triplet. Here, we demonstrate that the doublet inhibited the progression of HGF-overexpressing *EGFR*-mutant lung cancer more efficiently than the clinically available triplet treatment. Moreover, TAS-115 combined with erlotinib also controlled tumor growth well and, remarkably, delayed regrowth even after cessation of the treatment.

Materials and Methods

Cell cultures and reagents

The *EGFR*-mutant human lung adenocarcinoma cell lines PC-9 (del E746_A750) and HCC827, with deletions in *EGFR* exon 19, were purchased from Immuno-Biological Laboratories Co. and from American Type Culture Collection, respectively (21). Human *HGF*-gene transfectant (PC-9/HGF) and vector control (PC-9/Vec) cells were established as previously described (24). These cell lines were maintained in RPMI-1640 medium supplemented with 10% FBS and antibiotics. All cells were passaged for less than 3 months before renewal from frozen, early-passage stocks. The human embryonic lung fibroblast cell line MRC-5 was purchased from the Health Science Research Resources Bank (Osaka, Japan). MRC-5 (P30–35) cells were maintained in Dulbecco's modified Eagle's medium with 10% FBS, 100 units/mL penicillin, 100 μg/mL streptomycin. Human dermal microvascular endothelial cells (HMVECs) were incubated in RPMI-1640 medium with 10% FBS (control), RPMI-1640 medium with 10% FBS plus VEGF, or HuMedia-MvG with different concentrations of TAS-115 for 72 hours. Thereafter, cell viability was determined by MTT assay. Cells were regularly screened for mycoplasma by using MycoAlert Mycoplasma Detection Kits (Lonza, Rockland, ME). The cell lines were authenticated at the laboratory of the National Institute of Biomedical Innovation (Osaka, Japan) by short tandem repeat analysis. TAS-115 was synthesized by Taiho Co., Ltd. Erlotinib and crizotinib were obtained from Selleck Chemicals (Houston, TX). Bevacizumab was obtained from Chugai Pharma (Tokyo, Japan). Human recombinant HGF was prepared as previously described (24).

Production of HGF and VEGF in cell culture supernatants

Cells (2×10^5) were cultured in 2 mL of culture medium with 10% FBS for 24 hours, washed with PBS, and incubated for 48 hours in the medium supplemented with 10% FBS. In some experiments, HGF was added to the medium. The culture media was harvested and centrifuged, and the supernatants were stored at –80°C until analysis. The concentrations of HGF and VEGF were determined by IMMUNIS HGF EIA (Institute of Immunology, Tokyo, Japan) or Quantikine VEGF ELISA (R&D Systems, Minneapolis, MN), respectively, according to the respective manufacturer's protocol. All samples were run in duplicate. Color intensity was measured at 450 nm by using a spectrophotometric plate reader. Growth factor concentrations were determined by comparison with standard curves. The detection limits for HGF and VEGF were 100 pg/mL and 31 pg/mL, respectively.

Cell viability assay

Cell growth was measured using the MTT dye reduction method (24). Tumor cells were plated into 96-well plates at a density of 2×10^3 cells/100 mL RPMI-1640 medium with 10% FBS per well. After 24-hour incubation, various reagents were added to each well, and the cells incubated for a further 72 hours, followed by the addition of 50 µL of MTT solution (2 mg/mL; Sigma, St. Louis, MO) to each well and incubation for 2 hours. The media containing MTT solution was removed, and the dark blue crystals were dissolved by adding 100 mL of dimethyl sulfoxide. The absorbance of each well was measured with a microplate reader at test and reference wavelengths of 550 and 630 nm, respectively. The percentage of growth is shown relative to untreated controls. Each reagent concentration was tested at least in triplicate during each experiment, and each experiment was conducted at least 3 times.

Antibodies and western blotting

Protein aliquots of 25 µg each were resolved by SDS-polyacrylamide gel (Bio-Rad, Hercules, CA) electrophoresis and transferred to polyvinylidene difluoride membranes (Bio-Rad). After washing 4 times, the membranes were incubated with Blocking One (Nacalai Tesque, Kyoto, Japan) for 1 hour at room temperature and overnight at 4°C with primary antibodies to ß-actin (13E5), Met (25H2), phospho-Met (Y1234/Y1235;3D7), phospho-EGFR (Y1068), Akt, phospho-Akt (Ser473; 736E11), VEGFR-2 (55B11), phospho-VEGFR-2 (Tyr951;15D2), human EGFR (1 µg/mL), human/mouse/rat Erk1/Erk2 (0.2 µg/mL), and p-Erk1/Erk2 (T202/Y204; 0.1 µg/mL; R&D Systems). After 3 washes, the membranes were incubated for 1 hour at room temperature with species-specific, horseradish peroxidase-conjugated secondary antibodies. Immunoreactive bands were visualized with Super Signal West Dura Extended Duration Substrate (Thermo Fisher Scientific, Waltham, MA), an enhanced chemiluminescence substrate (Pierce Biotechnology, Rockfold, IL). Each experiment was conducted at least 3 times independently.

Co-culture of lung cancer cells with fibroblasts or endothelial cells

Cells were co-cultured in Transwell collagen–coated chambers separated by an 8-mm (BD Biosciences, San Jose, CA) or 3-mm (Corning, Tewksbury, MA) pore size filter. Tumor cells (8×10^3 cells/800 mL) with or without TAS-115 (1.0 µmol/L) or erlotinib (0.3 µmol/L) in the lower chamber were co-cultured with MRC-5 (1×10^4 cells/300 µL) cells in the upper chamber for 72 hours. The upper chamber was then removed, 200 µL of MTT solution was added to each well, and the cells were incubated for 2 hours at 37°C.

The media was removed, and the dark blue crystals in each well were dissolved in 400 µL of dimethyl sulfoxide. Absorbance was measured with an MTP-120 Microplate reader (Corona Electric, Ibaraki, Japan) at test and reference wavelengths of 550 and 630 nm, respectively. The percentage of growth was measured relative to untreated controls. All samples were assayed at least in triplicate, with each experiment conducted 3 times independently.

Subcutaneous xenograft models

Nude mice (male, 5–6 weeks old) were obtained from Clea (Tokyo, Japan). Cultured tumor cells (PC-9/Vec or PC-9/HGF) were implanted subcutaneously into the flanks of each mouse at 3×10^6 cells/0.1 mL. When tumor volumes reached 100–200 mm^3, the mice (n = 5 per group) were randomized to the following groups: (a) no treatment (control group), (b) only 50 mg/kg of erlotinib orally, (c) only 25 mg/kg of crizotinib orally, (d) only 100 µg/mouse of bevacizumab intraperitoneally, (e) only 75 mg/kg of TAS-115 orally, (f) erlotinib and crizotinib, (g) crizotinib and bevacizumab, (h) erlotinib and bevacizumab, (i) erlitinib, crizotinib, and bevacizumab, and (j) erlotinib and TAS-115. Each tumor was measured in 2 dimensions 3 times a week, and the volume was calculated using the following formula: tumor volume (mm^3) = 1/2(length (mm) × (width (mm))^2). All animal experiments complied with the Guidelines for the Institute for Experimental Animals, Kanazawa University Advanced Science Research Center (Approval No. AP-122505).

Histological analyses

For detection of endothelial cells (CD31), 5-µm-thick frozen sections of xenograft tumors were fixed with cold acetone and washed with PBS. Then, endogenous peroxidase activity was blocked by incubation in 3% aqueous H_2O_2 for 10 min. Following treatment with 5% normal horse serum, the sections were incubated with primary antibodies to mouse CD31 (MEC13.3; BD Biosciences). After probing with species-specific, biotinylated secondary antibodies, the sections were incubated for 30 min with avidin–biotinylated peroxidase complex (ABC) by using a Vectastain ABC kit (Vector Laboratories, Burlingame, CA). The DAB (3,3′-diaminobenzidine tetrahydrochloride) Liquid System (DAKO, Glostrup, Denmark) was used to detect immunostaining. Omission of the primary antibody served as a negative control. Terminal deoxynucleotidyl transferase–mediated nick end labeling (TUNEL) staining was performed using the Apoptosis Detection System (Promega Corporation, Madison, WI). Briefly, 5-µm-thick frozen sections of xenograft tumors were fixed with PBS containing 4% formalin. The slides were washed with PBS and permeabilized with 0.2% Triton X-

100. The samples were then equilibrated, and DNA strand breaks were labeled with fluorescein-12-2-deoxy-uridine-5-triphosphate (fluorescein-12-dUTP) by adding the nucleotide mixture and the terminal deoxynucleotidyl transferase enzyme. The reaction was stopped with saline sodium citrate, and the localized green fluorescence of apoptotic cells was detected by fluorescence microscopy (200x). The 5 areas containing the highest numbers of stained cells within a section were selected for histologic quantitation by light or fluorescent microscopy at a 400-fold magnification. All results were independently evaluated by 3 investigators (J.N., T.N, and S.T.).

Statistical analysis

Differences were analyzed by one-way ANOVA. All statistical analyses were carried out using GraphPad Prism Ver. 4.01 (GraphPad Software, Inc., La Jolla, CA). A *P*-value of <0.01 was considered statistically significant.

Results

Effect of crizotinib and TAS-115 on bypass resistance signals triggered by exogenous HGF *in vitro*

In the first set of experiments, we examined the effect of crizotinib and TAS-115 on exogenously added HGF-triggered EGFR-TKI resistance *in vitro*. PC-9 and HCC827 cells are highly sensitive to erlotinib, whereas exogenously added HGF induces resistance to erlotinib in both cell lines. Crizotinib on its own discernibly inhibits the growth of PC-9 cell at high concentrations, consistent with its multikinase activities, and it remarkably sensitizes the cell to erlotinib even in the presence of HGF. TAS-115 does not affect the growth of PC-9 or HCC827 cells at concentrations less than 10 μmol/L; however, the combined use of TAS-115 with erlotinib reverses HGF-induced resistance in the cell lines in a concentration-dependent manner (Fig. 1A, B, Fig. 2A, B, and Supplemental Figure 2). We previously reported that stromal fibroblasts are a source of exogenous HGF for EGFR-TKI naive NSCLC and that fibroblast-derived HGF induces resistance to gefitinib and erlotinib in PC-9 and HCC827 cells (25). Crizotinib and TAS-115 reverse the erlotinib resistance of PC-9 cells induced by co-culturing with MRC-5 cells (Supplemental Figure 3A, B). These results indicate that both crizotinib and TAS-115 can reverse the EGFR-TKI resistance induced by exogenous HGF *in vitro*.

Effect of crizotinib and TAS-115 on bypass resistance signals triggered by endogenous HGF

Previously we showed that HGF is predominantly present in tumor cells of NSCLC patients with acquired resistance to EGFR-TKIs and that transient *HGF*-gene transfection into PC-9 cells results in resistance to EGFR-TKIs (20). We, therefore, generated a stable *HGF*-gene transfectant in PC-9 cells (PC-9/HGF) and assessed the effects against continuously produced endogenous HGF. PC-9/HGF cells secrete high levels of HGF and become resistant to erlotinib, whereas PC-9 or the vector control PC-9/Vec cells do not. Although TAS-115 does not affect the growth of PC-9/HGF cells, crizotinib discernibly inhibits it at high concentrations. The combination of crizotinib or TAS-115 with erlotinib successfully reverses the resistance of PC-9/HGF cells (Fig. 2A–G). Using western blotting, we examined the effects of crizotinib and TAS-115 on signal transduction in PC-9/Vec and PC-9/HGF cells (Fig. 2H–I). We found that erlotinib inhibits the phosphorylation of EGFR and ErbB3 in PC-9/Vec cells, thereby inhibiting the phosphorylation of Akt and ERK1/2. Met phosphorylation is observed in PC-9/HGF cells but not in PC-9/Vec cells. However, erlotinib fails to inhibit phosphorylation of Akt or Erk1/2 in the presence of HGF. Both crizotinib and TAS-115

suppress the constitutive phosphorylation of Met but not EGFR, ErbB3, or downstream Akt and ERK1/2. HGF stimulates the phosphorylation of Met, but the combined use of crizotinib or TAS-115 with erlotinib inhibits the phosphorylation of Met, Akt, and Erk1/2. These results suggest that crizotinib and TAS-115, when combined with erlotinib, reverse HGF-triggered erlotinib resistance by inhibiting the Met/Gab1/PI3K/Akt pathway.

Effect of crizotinib and TAS-115 on angiogenesis *in vitro* and *in vivo*

As we reported previously (21), exogenous and endogenous HGF stimulated VEGF production in the PC-9 cancer cell line. Both crizotinib and TAS-115 inhibit VEGF production, presumably due to inhibiting Met activation by HGF (Fig. 3A, B). We also assessed the effect of crizotinib, TAS-115, and bevacizumab on the growth of HMVECs. VEGF promoted HMVEC viability, whereas TAS-115 and bevacizumab, but not crizotinib, inhibits VEGF-stimulated viability of HMVECs in a dose-dependent manner (Fig. 3C, D). We also explored the potential of TAS-115 against VEGFR-2. Western blot analysis indicated that VEGFR-2 is phosphorylated by VEGF stimulation in HMVECs, and TAS-115 and bevacizumab show an inhibitory effect (Supplemental Figure 4). We next examined the effect on *in vivo* angiogenesis by using short term treatment models. Nude mice with established subcutaneous tumors (tumor volume ~100 mm^3) were treated with erlotinib with or without crizotinib, bevacizumab, and/or TAS-115, and tumor vascularization was determined on day 4 (Fig. 4A, B). In PC-9/Vec tumors, treatment with erlotinib alone, TAS-115 alone, or erlotinib with TAS-115 inhibited vascularization. PC-9/HGF tumors have more vascularization than PC-9/Vec tumors. In PC-9/HGF tumors, treatment with bevacizumab, but not erlotinib or crizotinib, inhibited vascularization. We found that TAS-115 inhibited vascularization more potently than bevacizumab. Under these experimental conditions, treatment with erlotinib plus crizotinib inhibited vascularization. Importantly, erlotinib plus TAS-115 more potently inhibited vascularization, compared with erlotinib plus crizotinib, with or without bevacizumab. These results indicate that TAS-115 has a high potential to inhibit angiogenesis *in vivo* in *EGFR*-mutant tumors that produce high levels of HGF. We also confirmed that treatment with crizotinib or TAS-115 inhibits the phosphorylation of EGFR and Met *in vivo* (Supplemental Figure 5).

Effect of combined treatment on growth of HGF-overexpressing tumors *in vivo*.

Nude mice bearing established subcutaneous tumors (tumor volume ~100 mm^3) were treated with erlotinib with or without crizotinib, bevacizumab, and/or TAS-115 for 39

days. The treatment was feasible, and no adverse events, including loss of weight, were observed. Tumor volumes on day 39 are shown in Fig 5A and B. Erlotinib markedly inhibited the growth of PC-9/Vec tumors, but TAS-115 inhibited it only modestly (81.7% and 40%, respectively). In PC-9/HGF tumors, erlotinib alone and crizotinib alone inhibited tumor growth only slightly (30% and 31.9%, respectively). Moreover, bevacizumab alone and TAS-115 alone inhibited tumor growth modestly (67% and 76.6%, respectively). Erlotinib plus crizotinib, with or without bevacizumab, inhibited tumor growth markedly (87.1% and 88.3%, respectively). Importantly, erlotinib plus TAS-115 further inhibited tumor growth significantly (93.7%).

Effect of combined treatment on regrowth of HGF-overexpressing tumors after cessation of the treatment.

We further evaluated the effect on regrowth of PC-9/HGF tumors after cessation of drug treatment. After 10 days of cessation, tumors treated with erlotinib plus crizotinib with or without bevacizumab regrew to 4.5 and 3.3 times their initial size at the start of cessation, respectively. Tumors treated with erlotinib plus TAS-115 re-grew to only 1.7 times their initial size (Fig 6A). To explore the mechanism of this phenomenon, we again evaluated tumor vascularization on day 49 (10 days after the start of cessation). Consistent with an inhibitory effect against tumor regrowth, vessel density was high (104.6 ± 7.3) and modest (68.6 ± 8.0) in tumors treated with erlotinib plus crizotinib without and with bevacizumab, respectively, whereas vessel density in the tumors treated with erlotinib plus TAS-115 was very low (37.8 ± 3.5; Fig 6B). However, the number of apoptotic cells was low (1.5 ± 0.6), modest (7.3 ± 5.7), and high (22.7 ± 6.4) in the tumors treated with erlotinib plus crizotinib, crizotinib and bevacizumab, and TAS-115, respectively. These results suggest that erlotinib plus TAS-115 prevents tumor regrowth, even after cessation, via sustained inhibition of angiogenesis.

Discussion

In the present study, we demonstrated that combined use of erlotinib and TAS-115, a novel angiogenesis inhibitor with Met inhibitory activity, as well as the use of a triplet of clinically available drugs (erlotinib, crizotinib, and bevacizumab), could inhibit the growth of HGF-triggered EGFR-TKI-resistant tumors containing *EGFR* mutations. Moreover, TAS-115 combined with erlotinib remarkably delayed the regrowth of the HGF-triggered EGFR-TKI-resistant tumors.

Since we reported that HGF is a resistance factor to EGFR-TKI in *EGFR*-mutant lung cancer (9), HGF has been shown to induce resistance to various molecularly targeted drugs in different types of cancers with driver oncogenes. HGF causes resistance to a selective ALK inhibitor (26) and a BRAF inhibitor (27) in lung cancer with *ALK* rearrangement and melanoma with *BRAF* mutation, respectively, by inducing bypass signals that trigger resistance. Moreover, HGF restores angiogenesis associated with Met expression in tumor vascular endothelial cells and thus induces resistance to sunitinib in various types of cancer (28). These observations indicate that HGF induces resistance to molecularly targeted drugs by multiple mechanisms; therefore, it is an important therapeutic target for circumventing resistance to various molecularly targeted drugs.

HGF and its receptor Met have a close relationship with VEGF. Anti-VEGF treatment resulted in a remarkable upregulation of Met expression in tumors (29). Hypoxia-stimulated expression of VEGF (30), Met (29), and Neuropilin1 (NRP1), a receptor of VEGF, promotes tumor progression (29, 31). Furthermore, it was reported that serum levels of HGF and VEGF were inversely correlated with the clinical response to EGFR-TKIs in lung cancer (32–34). In addition, a dual inhibitor of VEGFR-2 and Met (XL-184) was shown to have completely suppressed invasion and metastasis in a pancreatic cancer model *in vivo* (29). These studies indicate the rationale for simultaneous inhibition of the HGF-Met and VEGF/VEGFR-2 axes for cancer therapy.

In line with our previous results, we observed that inhibition of both the driver signal (EGFR) and the resistance signal (Met) remarkably suppressed the growth of HGF-triggered EGFR-TKI-resistant tumors *in vivo*. However, the tumors regrew immediately after the cessation of the dual inhibition, which indicated the presence of cancer cells with proliferating potential that persisted continuously throughout the dual inhibition. Mechanisms of the resistance to dual inhibition should be clarified in the near future.

Additional inhibition of angiogenesis by VEGF neutralization or VEGFR inhibition in addition to dual inhibition (EGFR and Met) could further inhibit growth of HGF-

triggered EGFR-TKI resistant tumor and delay regrowth of the tumors after cessation of the treatment. Bevacizumab in combination with cytotoxic chemotherapy has been shown to prolong progression-free survival in various solid tumors. Our results suggest that the angiogenesis inhibitor in combination with molecularly targeted drugs such as EGFR-TKI and Met-TKI, which directly act on cancer cells, may also delay tumor progression.

It is still controversial whether tumor blood vessels rapidly regrow after cessation of VEGF inhibition. Mancuso et al reported that tumor vasculature regrew within 7 days of cessation of VEGFR inhibitors (given for 7 days) in the RIP-Tag2 pancreatic cancer model and the Lewis lung carcinoma-xenograft model (35). Bagri et al. showed that long-term (7 weeks) treatment with anti-VEGF antibody prevented the regrowth of tumors compared with control or short-term (2 weeks) treatment, but the effect of the long-term treatment on vasculature regrowth after cessation was not well elucidated (36). In the present study, we demonstrated that regrowth of tumor vasculature was inhibited even after cessation for 10 days of treatment when, prior to that, continuous treatment (for 39 days) consisted of bevacizumab plus erlotinib and crizotinib or TAS-115 plus erlotinib; and this inhibition was associated with a high number of apoptotic cells in the tumors and delayed tumor regrowth. These effects were more remarkable with TAS-115 plus erlotinib than with the triplet treatment in our experimental conditions. It is unclear why continuous triple inhibition, especially by TAS-115 plus erlotinib, delayed the recovery of tumor angiogenesis. One possible explanation is that continuous treatment with TAS-115 may impair the function of endothelial progenitor cells expressing VEGFR-2. Further studies with longer follow-up and histochemical analysis will be required to determine the exact mechanisms.

Inhibition of multiple signaling pathways may cause severe adverse events, especially with continuous admiration of the inhibitors. In our study, 50 mg/kg erlotinib administered daily plus 100 μg/body bevacizumab administered weekly did not show obvious adverse events in nude mice. However, some nude mice treated with daily 50 mg/kg crizotinib plus daily 50 mg/kg erlotinib exhibited severe weight loss and died. Thus, we had to reduce the dose of crizotinib to 25 mg/kg daily when administered along with 50 mg/kg erlotinib. On the other hand, daily administration of 75 mg/kg TAS-115, as expected, inhibited its 2 targets, Met phosphorylation and angiogenesis, *in vivo*, and did not show obvious adverse events, including weight loss, even in combination with daily administration of 50 mg/kg erlotinib, suggesting the feasibility of this combined treatment. However, the safety and efficacy of triple inhibition with the triplet of clinically available drugs or with erlotinib plus TAS-115 need to be carefully evaluated

in clinical trials.

In conclusion, we demonstrated that triple inhibition of EGFR, Met, and angiogenesis could be achieved by a combination of clinically available drugs (erlotinib, crizotinib, and bevacizumab) or erlotinib and TAS-115 and that the triple inhibition efficiently controlled growth of HGF-triggered, EGFR-TKI-resistant tumors containing *EGFR* mutations. Clinical trials are warranted to evaluate the efficacy and safety of the triple inhibition in *EGFR*-mutant lung cancer patients who acquired EGFR-TKI resistance due to HGF.

Authors' Contributions

Conception and design: J. Nakade, S. Takeuchi, S. Yano

Development of methodology: J. Nakade, S. Takeuchi, S. Yano

Analysis and interpretation of data (e.g., statistical analysis, biostatistics, and computational analysis): J. Nakade, S. Takeuchi

Acquisition of data (provided animals, acquired and managed patients, provided facilities, etc.): J. Nakade, T. Nakagawa, D. Ishikawa, T. Sano, L. Zhao, S. Takeuchi

Writing, reviewing, and/or revising the manuscript: J. Nakade, S. Takeuchi, S. Yano

Administrative, technical, and material support (i.e., reporting or organizing data and constructing databases): J. Nakade, T. Nakagawa, S. Nanjo, T. Yamada, H. Ebi, K. Yasumoto, K. Matsumoto, K. Yonekura, S. Yano

Study supervision: S. Yano

References

1. Lynch TJ, Bell DW, Sordella R, et al. Activating mutations in the epidermal growth factor receptor underlying responsiveness of non-small-cell lung cancer to gefitinib. *N Engl J Med* 2004;350: 2129–39.

2. Paez JG, Jänne PA, Lee JC, et al. EGFR mutations in lung cancer: correlation with clinical response to gefitinib therapy. *Science* 2004;304:1497–1500.

3. Pao W, Miller V, Zakowski M, et al. EGF receptor gene mutations are common in lung cancers from "never smokers" and are associated with sensitivity of tumors to gefitinib and erlotinib. *Proc Natl Acad Sci USA* 2004;101:13306–11.

4. Jackman D, Pao W, Riely GJ, et al. Clinical definition of acquired resistance to epidermal growth factor receptor tyrosine kinase inhibitors in non-small-cell lung cancer. *J Clin Oncol* 2010;28:357–60.

5. Pao W, Chmielecki J. Rational, biologically based treatment of EGFR-mutant non-small-cell lung cancer. *Nat Rev Cancer* 2010;10:760–74.

6. Kobayashi S, Boggon TJ, Dayaram T, et al. EGFR mutation and resistance of non-small-cell lung cancer to gefitinib. *N Engl J Med* 2005;352:786–92.

7. Pao W, Miller VA, Politi KA, et al. Acquired resistance of lung adenocarcinomas to gefitinib or erlotinib is associated with a second mutation in the EGFR kinase domain. *PLoS Med* 2005;2:e73.

8. Engelman JA, Zejnullahu K, Mitsudomi T, et al. MET amplification leads to gefitinib resistance in lung cancer by activating ERBB3 signaling. *Science* 2007;316:1039–43.

9. Yano S, Wang W, Li Q, et al. Hepatocyte growth factor induces gefitinib resistance of lung adenocarcinoma with epidermal growth factor receptor-activating mutations. *Cancer Res* 2008;68: 9479-87.

10. Bivona TG, Hieronymus H, Parker J, et al. FAS and NF-κB signalling modulate dependence of lung cancers on mutant EGFR. *Nature* 2011;471:523–6.

11. Zhang Z, Lee JC, Lin L, et al. Activation of the AXL kinase causes resistance to EGFR-targeted therapy in lung cancer. *Nat Genet* 2012;44:852–60.

12. Zakowski MF, Ladanyi M, Kris MG. EGFR mutations in small-cell lung cancers in patients who have never smoked. *N Engl J Med* 2006;355:213–5.

13. Morinaga R, Okamoto I, Furuta K, et al. Sequential occurrence of non-small cell and small cell lung cancer with the same EGFR mutation. *Lung Cancer* 2007;58:411–3.

14. Shiao TH, Chang YL, Yu CJ, et al. Epidermal growth factor receptor mutations in small cell lung cancer: a brief report. *J Thorac Oncol* 2011;6:195–8.

15. Frederick BA, Helfrich BA, Coldren CD, et al. Epithelial to mesenchymal transition predicts gefitinib resistance in cell lines of head and neck squamous cell carcinoma and

non-small cell lung carcinoma. *Mol Cancer Ther* 2007; 6:1683–91.
16. Uramoto H, Iwata T, Onitsuka T, et al. Epithelial-mesenchymal transition in EGFR-TKI acquired resistant lung adenocarcinoma. *Anticancer Res* 2010;30:2513–7.
17. Suda K, Tomizawa K, Fujii M, et al. Epithelial to mesenchymal transition in an epidermal growth factor receptor-mutant lung cancer cell line with acquired resistance to erlotinib. *J Thorac Oncol* 2011;6:1152–61.
18. Garofalo M, Romano G, Di Leva G, et al. EGFR and MET receptor tyrosine kinase-altered microRNA expression induces tumorigenesis and gefitinib resistance in lung cancers. *Nat Med* 2011;18:74–82.
19. Huang S, Hölzel M, Knijnenburg T, et al. MED12 controls the response to multiple cancer drugs through regulation of TGF-β receptor signaling. *Cell* 2012;151:937–50
20. Yano S, Takeuchi S, Nakagawa T, et al. Ligand-triggered resistance to molecular targeted drugs in lung cancer: Roles of hepatocyte growth factor and epidermal growth factor receptor ligands. *Cancer Sci* 2012;103:1189–94.
21. Takeuchi S, Wang W, Li Q, et al. Dual inhibition of Met kinase and angiogenesis to overcome HGF-induced EGFR-TKI resistance in EGFR mutant lung cancer. *Am J Pathol* 2012;181:1034–43.
22. Kwak EL, Bang YJ, Camidge DR, et al. Anaplastic lymphoma kinase inhibition in non-small-cell lung cancer. *N Engl J Med* 2010;363:1693–703.
23. Bergethon K, Shaw AT, Ou SH, et al. ROS1 rearrangements define a unique molecular class of lung cancers. *J Clin Oncol* 2012;30:863–70.
24. Nakagawa T, Takeuchi S, Yamada T, et al. Combined therapy with mutant-selective EGFR inhibitor and Met kinase inhibitor for overcoming erlotinib resistance in EGFR-mutant lung cancer. *Mol Cancer Ther* 2012,11;2149–57.
25. Yamada T, Matsumoto K, Wang W, et al. Hepatocyte growth factor reduces susceptibility to an irreversible epidermal growth factor receptor inhibitor in EGFR-T790M mutant lung cancer. *Clin Cancer Res* 2010;16:174–83.
26. Yamada T, Takeuchi S, Nakade J, et al. Paracrine receptor activation by microenvironment triggers bypass survival signals and ALK inhibitor resistance in EML4-ALK lung cancer cells. *Clin Cancer Res* 2012;18:3592–602.
27. Wilson TR, Fridlyand J, Yan Y, et al. Widespread potential for growth-factor-driven resistance to anticancer kinase inhibitors. *Nature* 2012;487:505–9.
28. Shojaei F, Lee JH, Simmons BH, et al. HGF/c-Met acts as an alternative angiogenic pathway in sunitinib-resistant tumors. *Cancer Res* 2010;70:10090–100.
29. Sennino B, Ishiguro-Oonuma T, Wei Y, et al. Suppression of tumor invasion and metastasis by concurrent inhibition of c-Met and VEGF signaling in pancreatic

neuroendocrine tumors. *Cancer Discov* 2012;2:270–87.
30. Endoh H, Yatabe Y, Kosaka T, et al. PTEN and PIK3CA expression is associated with prolonged survival after gefitinib treatment in EGFR-mutated lung cancer patients. *J Thorac Oncol* 2006;1:629–34.
31. Zhang S, Zhau HE, Osunkoya AO, et al. Vascular endothelial growth factor regulates myeloid cell leukemia-1 expression through neuropilin-1-dependent activation of c-MET signaling in human prostate cancer cells. *Mol Cancer* 2010;9:9.
32. Kasahara K, Arao T, Sakai K, et al. Impact of serum hepatocyte growth factor on treatment response to epidermal growth factor receptor tyrosine kinase inhibitors in patients with non-small cell lung adenocarcinoma. *Clin Cancer Res* 2010;16:4616–24.
33. Tanaka H, Kimura T, Kudoh S, et al. Reaction of plasma hepatocyte growth factor levels in non-small cell lung cancer patients treated with EGFR-TKIs. *Int J Cancer* 2011;129:1410–6.
34. Han JY, Kim JY, Lee SH, et al. Association between plasma hepatocyte growth factor and gefitinib resistance in patients with advanced non-small cell lung cancer. *Lung Cancer* 2011;74:293–9.
35. Mancuso MR, Davis R, Norberg SM, et al. Rapid vascular regrowth in tumors after reversal of VEGF inhibition. *J Clin Invest* 2006; 116:2610–21.
36. Bagri A, Berry L, Gunter B, et al. Effects of anti-VEGF treatment duration on tumor growth, tumor regrowth, and treatment efficacy. *Clin Cancer Res* 2010;16:3887–900.

Figure Legends

Figure 1. Combined use of crizotinib or TAS-115 with erlotinib reverses resistance to EGFR-TKI induced by exogenous HGF. PC-9 cells were incubated with or without erlotinib or crizotinib and TAS-115 in the presence or absence of HGF (20 ng/mL) for 72 hours. Cell viability was determined by MTT assay. Bars show SD. The data shown are representative of 5 independent experiments with similar results. EGFR, epidermal growth factor receptor; EGFR-TKI, EGFR tyrosine kinase inhibitor; HGF, hepatocyte growth factor.

Figure 2. Combined use of crizotinib or TAS-115 with erlotinib reverses resistance to EGFR-TKI induced by endogenous HGF. **(A)** PC-9/Vec and PC-9/HGF cells were incubated with or without erlotinib for 72 hours. Cell viability was determined by MTT assay. Bars show SD. **(B, D)** PC-9/Vec and PC-9/HGF cells were treated with crizotinib or TAS-115 for 72 hours. **(C-G)** PC-9/Vec and PC-9/HGF cells were incubated with or without erlotinib (0.3 μmol/L) with or without crizotinib (0.3 μmol/L) and TAS-115 (1.0 μmol/L) for 72 hours. The data shown are from 3 independent experiments with similar results. **(H, I)** PC-9/HGF cells were incubated with TAS-115 (1.0 μmol/L) or crizotinib (0.3 μmol/L) and/or erlotinib (0.3 μmol/L) for 1 hour. Thereafter, cell lysates were harvested, and phosphorylation of the indicated proteins was determined by western blot analysis.

Figure 3. Crizotinib and TAS-115 inhibits VEGF production by cancer cells and endothelial proliferation. **(A, B)** Tumor cells were incubated with or without HGF (50 ng/mL) in the presence of different concentrations of crizotinib or TAS-115 for 48 hours. Thereafter, supernatants were harvested, and the number of tumor cells was counted. VEGF concentration in the supernatants was determined by ELISA. VEGF levels corrected by the tumor cell number are shown. **(C, D)** HMVECs were incubated in RPMI-1640 medium with 10% FBS (control) or RPMI-1640 medium with 10% FBS in the presence or absence of VEGF (50 ng/mL) with different concentrations of TAS-115, crizotinib, or bevacizumab for 72 hours. Thereafter, cell viability was determined by MTT assay. Bars show SD. The data shown are from 3 independent experiments with similar results. VEGF, vascular endothelial growth factor

Figure 4. Treatment with erlotinib plus TAS-115 inhibits angiogenesis in PC-9/HGF tumors *in vivo*. Nude mice bearing PC-9/Vec or PC-9/HGF tumors (approximately 100 mm^3 in size) were administered erlotinib and/or crizotinib and/or TAS-115 orally, once

daily for 4 days, and/or bevacizumab intraperitoneally only once. **(A)** The mice were sacrificed on day 4, and the tumors were harvested. **(B)** Numbers of tumor vessels (mean ± SE) determined by CD31 immunohistochemical staining are shown for groups containing 5 mice each. Representative graphs are shown. The data shown are representative of 2 independent experiments with similar results.

Figure 5. Treatment with erlotinib plus TAS-115 inhibits the growth of PC-9/HGF tumors *in vivo*. **(A, B)** Nude mice bearing PC-9/Vec or PC-9/HGF tumors (approximately 100 mm^3 in size) were administered erlotinib and/or crizotinib and/or TAS-115 orally once daily and/or bevacizumab intraperitoneally once a week. Tumor volume was measured using calipers. Mean ± SE tumor volumes on day 39 are shown for groups containing 5 mice each. The data shown are representative of 2 independent experiments with similar results.

Figure 6. Treatment with erlotinib plus TAS-115 prevents regrowth of PC-9/HGF tumors even after cessation of treatment. **(A)** Nude mice bearing PC-9/HGF tumors were treated as described in Fig. 5 until day 39. Thereafter, treatment was terminated, and tumor volume was measured until day 49. **(B)** The mice were sacrificed on day 49, and tumors were harvested. Tumor vessels and apoptotic cells were determined by CD31 immunohistochemical and TUNEL staining, respectively.

Figure 1.

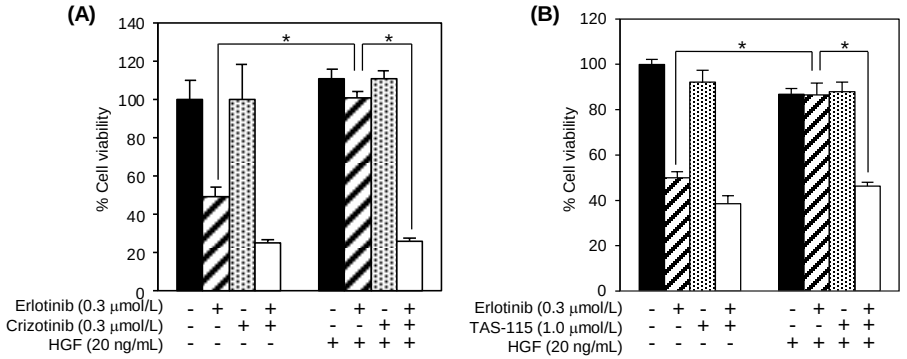

Figure 1. Combined use of crizotinib or TAS-115 with erlotinib reverses resistance to EGFR-TKI induced by exogenous HGF.

PC-9 cells were incubated with or without erlotinib or crizotinib and TAS-115 in the presence or absence of HGF (20 ng/mL) for 72 hours. Cell viability was determined by MTT assay. Bars show SD. The data shown are representative of 5 independent experiments with similar results. EGFR, epidermal growth factor receptor; EGFR-TKI, EGFR tyrosine kinase inhibitor; HGF, hepatocyte growth factor.

Figure 2.

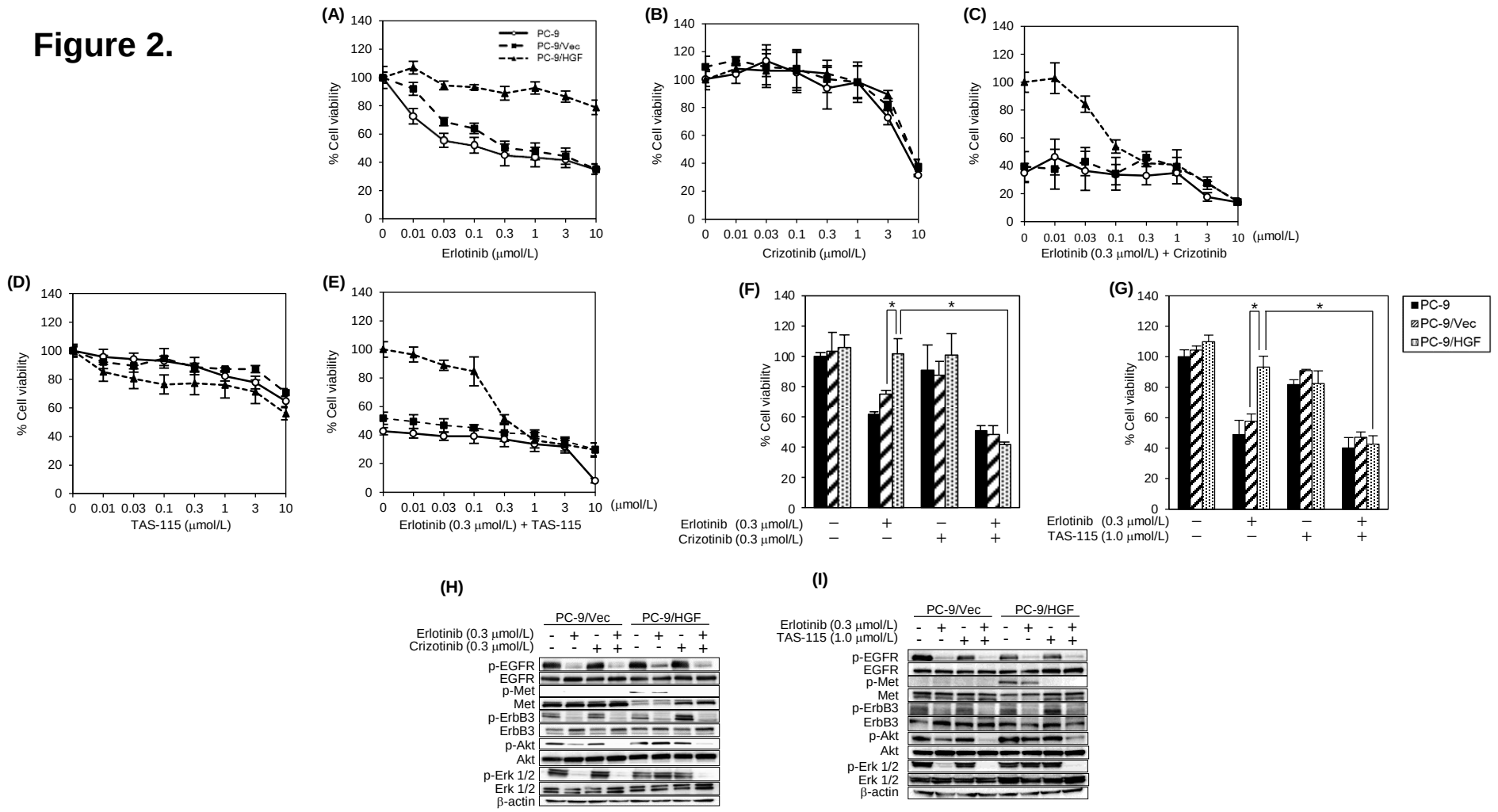

Figure 2. Combined use of crizotinib or TAS-115 with erlotinib reverses resistance to EGFR-TKI induced by endogenous HGF.

(A) PC-9/Vec and PC-9/HGF cells were incubated with or without erlotinib for 72 hours. Cell viability was determined by MTT assay. Bars show SD. **(B, D)** PC-9/Vec and PC-9/HGF cells were treated with crizotinib or TAS-115 for 72 hours. **(C-G)** PC-9/Vec and PC-9/HGF cells were incubated with or without erlotinib (0.3 μmol/L) with or without crizotinib (0.3 μmol/L) and TAS-115 (1.0 μmol/L) for 72 hours. The data shown are from 3 independent experiments with similar results. **(H, I)** PC-9/HGF cells were incubated with TAS-115 (1.0 μmol/L) or crizotinib (0.3 μmol/L) and/or erlotinib (0.3 μmol/L) for 1 hour. Thereafter, cell lysates were harvested, and phosphorylation of the indicated proteins was determined by western blot analysis.

Figure 3.

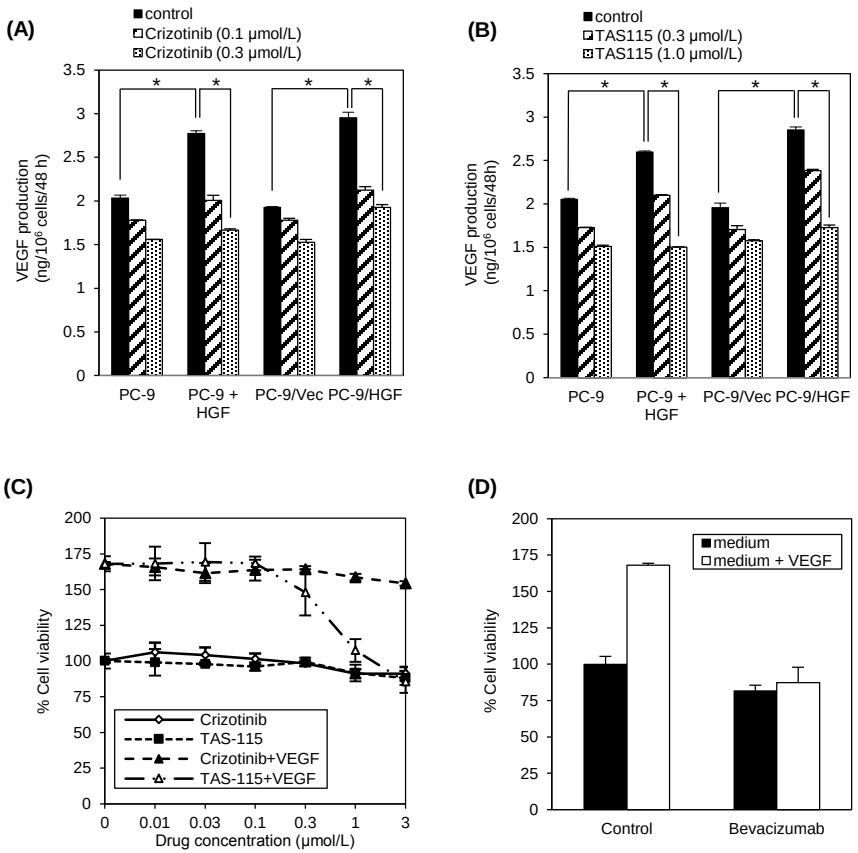

Figure 3. Crizotinib and TAS-115 inhibits VEGF production by cancer cells and endothelial proliferation.

(A, B) Tumor cells were incubated with or without HGF (50 ng/mL) in the presence of different concentrations of crizotinib or TAS-115 for 48 hours. Thereafter, supernatants were harvested, and the number of tumor cells was counted. VEGF concentration in the supernatants was determined by ELISA. VEGF levels corrected by the tumor cell number are shown. **(C, D)** HMVECs were incubated in RPMI-1640 medium with 10% FBS (control) or RPMI-1640 medium with 10% FBS in the presence or absence of VEGF (50 ng/mL) with different concentrations of TAS-115, crizotinib, or bevacizumab for 72 hours. Thereafter, cell viability was determined by MTT assay. Bars show SD. The data shown are from 3 independent experiments with similar results. VEGF, vascular endothelial growth factor

Figure 4.

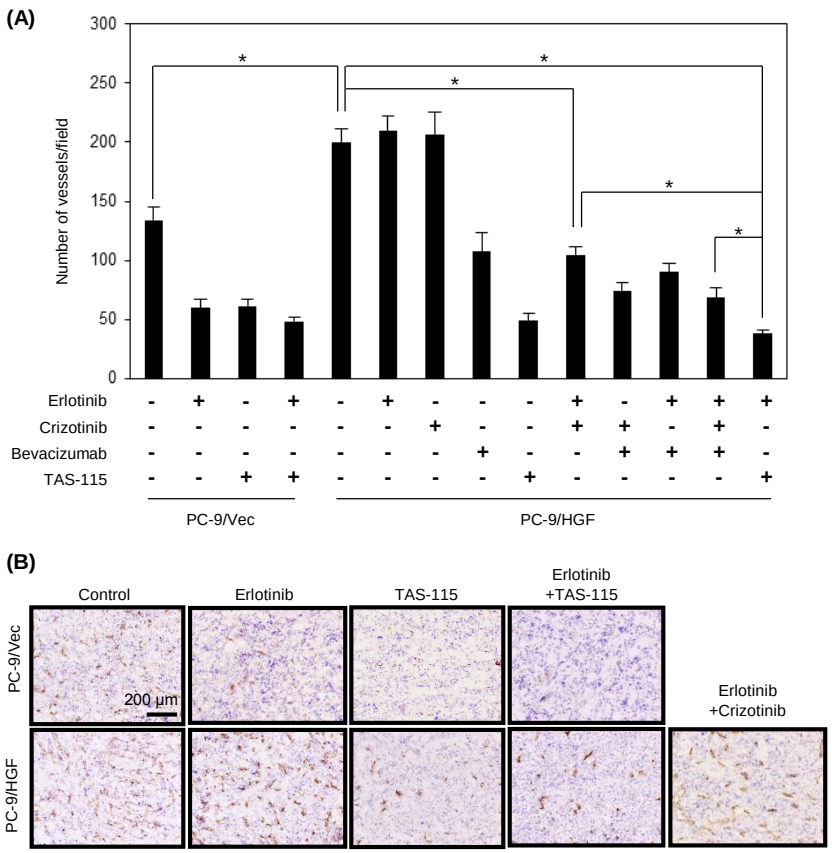

Figure 4. Treatment with erlotinib plus TAS-115 inhibits angiogenesis in PC-9/HGF tumors *in vivo*.

Nude mice bearing PC-9/Vec or PC-9/HGF tumors (approximately 100 mm^3 in size) were administered erlotinib and/or crizotinib and/or TAS-115 orally, once daily for 4 days, and/or bevacizumab intraperitoneally only once. **(A)** The mice were sacrificed on day 4, and the tumors were harvested. **(B)** Numbers of tumor vessels (mean ± SE) determined by CD31 immunohistochemical staining are shown for groups containing 5 mice each. Representative graphs are shown. The data shown are representative of 2 independent experiments with similar results.

Figure 5.

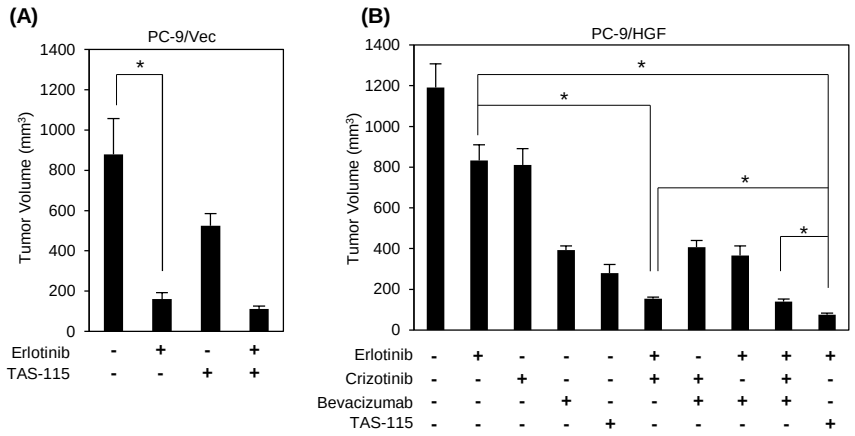

Figure 5. Treatment with erlotinib plus TAS-115 inhibits the growth of PC-9/HGF tumors *in vivo*.

(A, B) Nude mice bearing PC-9/Vec or PC-9/HGF tumors (approximately 100 mm^3 in size) were administered erlotinib and/or crizotinib and/or TAS-115 orally once daily and/or bevacizumab intraperitoneally once a week. Tumor volume was measured using calipers. Mean ± SE tumor volumes on day 39 are shown for groups containing 5 mice each. The data shown are representative of 2 independent experiments with similar results.

Figure 6.

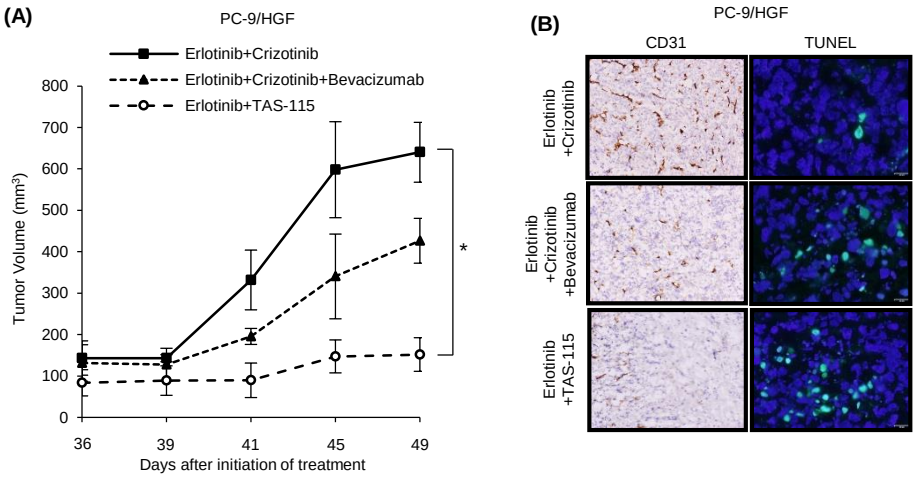

Figure 6. Treatment with erlotinib plus TAS-115 prevents regrowth of PC-9/HGF tumors even after cessation of treatment.

(A) Nude mice bearing PC-9/HGF tumors were treated as described in Fig. 5 until day 39. Thereafter, treatment was terminated, and tumor volume was measured until day 49. **(B)** The mice were sacrificed on day 49, and tumors were harvested. Tumor vessels and apoptotic cells were determined by CD31 immunohistochemical and TUNEL staining, respectively.

Supplemental Figure 1

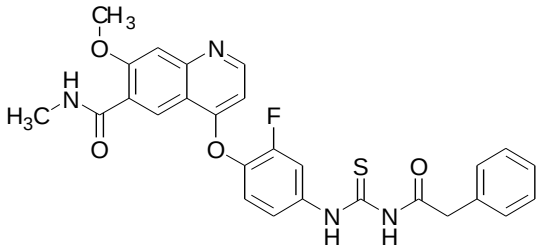

Supplemental Figure 1. Chemical structure of TAS-115.
4-[2-fluoro-4-[[[(2-phenylacetyl)amino]thioxomethyl]amino]phenoxy]-7-methoxy-N-methyl-6-quinolinecarboxamide.

Supplemental Figure 2

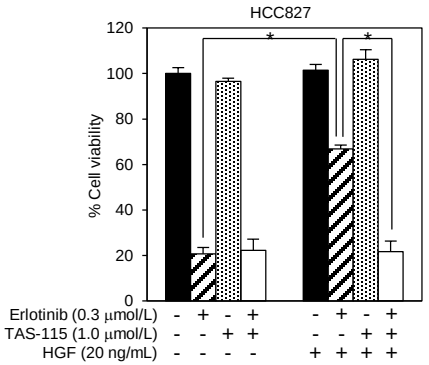

Supplemental Figure 2. Combined use of TAS-115 with erlotinib reverses resistance to EGFR-TKI induced by exogenous HGF on HCC827 cell.
HCC827 cells were incubated with or without erlotinib alone or erlotinib with TAS-115 in the presence or absence of HGF (20 ng/mL) for 72 hours. Thereafter, cell viability was determined by MTT assay. Bars show SD. The data shown are representative of 5 independent experiments with similar results.

Supplemental Figure 3

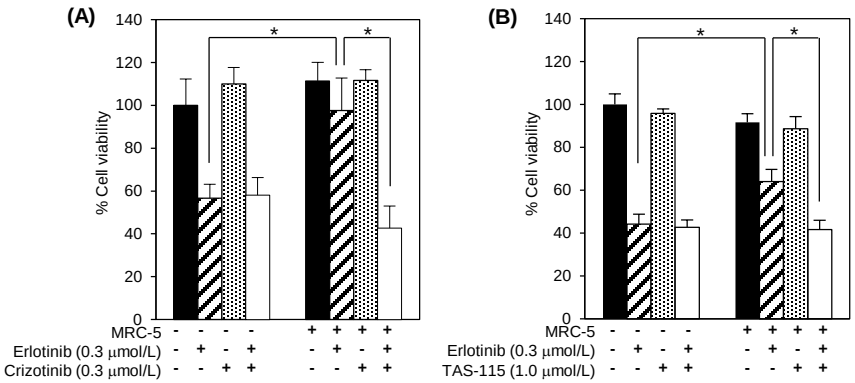

Supplemental Figure 3. Combined use of crizotinib or TAS-115 with erlotinib reverses resistance to EGFR-TKI induced by exogenous HGF secreted from MRC-5. We previously reported that human embryonic lung fibroblasts (MRC-5) produce HGF (25).The lung cancer cell line PC-9 was co-cultured with MRC-5 cells in the presence or absence of erlotinib (0.3 μmol/L) and/or crizotinib (0.3 μmol/L) and/or TAS-115 (1.0 μmol/L) for 72 hours, and cancer cell growth was determined by MTT assay.

Supplemental Figure 4

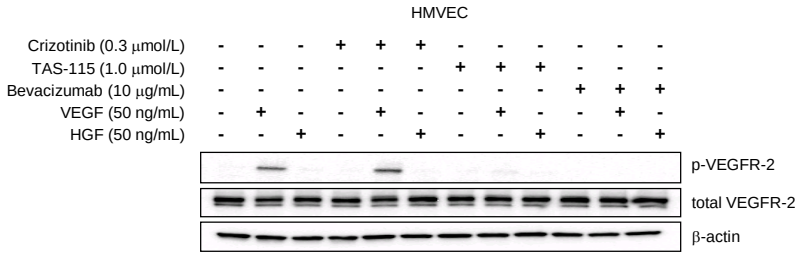

Supplemental Figure 4. Treatment with erlotinib plus TAS-115 inhibits phosphorylation of VEGFR-2 *in vivo*.
HMVECs were cultured with or without crizotinib (0.3 μmol/L) or TAS-115 (1.0 μmol/L) or bevacizumab (10 μg/mL) for 1 hour, and then 50 ng/mL of VEGF or HGF were added. After 10 min, the cells were lysed, and the indicated proteins were detected by western blot analysis.

Supplemental Figure 5

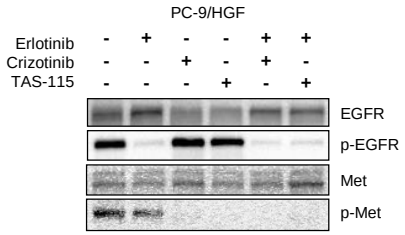

Supplemental Figure 5. Inhibitory effect of crizotinib or TAS-115 on EGFR or Met phosphorylation *in vivo*.
Nude mice bearing PC-9/HGF tumors were orally administered erlotinib (50 mg/kg) and/or crizotinib (25 mg/kg) and/or TAS-115 (75 mg/kg) or the vehicle, once daily. On day 4, 4 hours after treatment, the mice were sacrificed, and the tumors were resected. The amount of phosphorylated EGFR or Met and total EGFR or Met levels were determined by western blot analysis.